Faraday Discussions

Cite this: *Faraday Discuss.*, 2022, **235**, 36

ROYAL SOCIETY OF CHEMISTRY

PAPER

View Article Online
View Journal | View Issue

# Solvent-mediated isotope effects strongly influence the early stages of calcium carbonate formation: exploring $D_2O$ *vs.* $H_2O$ in a combined computational and experimental approach†

Michael King, ‡[a] Jonathan T. Avaro,‡[ab] Christine Peter,[a] Karin Hauser [a] and Denis Gebauer *[c]

Received 26th October 2021, Accepted 7th December 2021
DOI: 10.1039/d1fd00078k

In experimental studies, heavy water ($D_2O$) is employed, *e.g.*, so as to shift the spectroscopic solvent background, but any potential effects of this solvent exchange on reaction pathways are often neglected. While the important role of light water ($H_2O$) during the early stages of calcium carbonate formation has been realized, studies into the actual effects of aqueous solvent exchanges are scarce. Here, we present a combined computational and experimental approach to start to fill this gap. We extended a suitable force field for molecular dynamics (MD) simulations. Experimentally, we utilised advanced titration assays and time-resolved attenuated total reflection Fourier transform infrared (ATR-FTIR) spectroscopy. We find distinct effects in various mixtures of the two aqueous solvents, and in pure $H_2O$ or $D_2O$. Disagreements between the computational results and experimental data regarding the stabilities of ion associates might be due to the unexplored role of HDO, or an unprobed complex phase behaviour of the solvent mixtures in the simulations. Altogether, however, our data suggest that calcium carbonate formation might proceed "more classically" in $D_2O$. Also, there are indications for the formation of new structures in amorphous and crystalline calcium carbonates. There is huge potential towards further improving the understanding of mineralization mechanisms by studying solvent-mediated isotope effects, also beyond calcium carbonate. Last, it must be appreciated that $H_2O$ and $D_2O$ have significant, distinct effects on mineralization mechanisms, and that care has to be taken when experimental data from $D_2O$ studies are used, *e.g.*, for the development of $H_2O$-based computer models.

[a]*Department of Chemistry, University of Konstanz, Universitätsstr. 10, 78457 Konstanz, Germany*
[b]*Empa, Lerchenfeldstrasse 5, 9014 St. Gallen, Switzerland*
[c]*Institute of Inorganic Chemistry, Leibniz University of Hannover, Callinstr. 9, 30167 Hannover, Germany. E-mail: gebauer@acc.uni-hannover.de*

† Electronic supplementary information (ESI) available. See DOI: 10.1039/d1fd00078k

‡ These authors contributed equally and retain the right to list their names first in their respective CVs.

 

# Introduction

Deuteration of compounds is often employed to investigate reaction mechanisms based on the so-called kinetic isotope effect,[1] where doubling of the masses due to the change from hydrogen (H) to deuterium (D) reduces the vibrational frequency of the involved bonds.[2,3] This effect also allows shifting the vibrational modes of the aqueous solvent background in IR spectroscopic studies to explore, *e.g.*, protein dynamics.[4–7] In proton nuclear magnetic resonance spectroscopy, for instance, replacing $H_2O$ by $D_2O$ allows one to get rid of unwanted solvent resonance.[8] However, when changing the solvent from light to heavy water, also thermodynamic effects have to be considered.[9] Not only quantum nuclear effects but also electronic effects come into play and affect a variety of properties.[10] The O–D bond is shorter than the O–H bond, *i.e.*, 0.985(5) Å *vs.* 0.990(5) Å,[11,12] rendering the average number of hydrogen bonds within the bulk of $D_2O$ slightly higher.[13] Also, the peaks in the radial distribution function are more pronounced in the case of $D_2O$.[14] Thus, $D_2O$ is more ordered than $H_2O$.[14–17] This, in turn, causes different macroscopic and microscopic properties of these aqueous solvents. For example, the compressibility and polarizability of $D_2O$ are higher than those of $H_2O$.[18] Some further selected differences can be found in Table 1, and more details in ref. 9, 19 and 20.

The different properties of $D_2O$ also have consequences for solutes in heavy water. The neutral pH value of water increases from 7.0 to ~7.4 when changing from $H_2O$ to $D_2O$.[21,22] Also, the p$K_a$ value of acids shifts by an increment in the range of 0.5–0.7 in $D_2O$ with respect to the value in $H_2O$, *e.g.*, for the second deprotonation step of carbonic acid $pK_a^D - pK_a^H = 0.60$,[23] or 0.741.[21] Even deuteration of aliphatic C-atoms near a carboxyl group (*i.e.*, of C-alpha or C-beta atoms) affects the p$K_a$ value of the corresponding acids.[26]

The higher solubility of hydrocarbons and noble gases in $D_2O$[2,27,28] can be attributed to its higher compressibility (Table 1),[29] reflecting the ability to form nano-cavities more easily than light water. This also leads to a higher hydrophobicity of $D_2O$, even overcoming the opposing effect of stronger hydrogen bonds than in light water.[30] This effect, however, depends on solute size, shape and charge and can switch from attractive to repulsive.[29] The differences between light and heavy water can furthermore affect the stability of proteins, *i.e.*, the melting temperatures of some proteins in heavy water increase relative to $H_2O$.[31]

Table 1 Comparison of selected properties of light and heavy water

| | $H_2O$ | $D_2O$ |
|---|---|---|
| Melting point (101.325 kPa) [°C][19] | 0.00 | 3.82 |
| Boiling point (101.325 kPa) [°C][19] | 100.00 | 101.42 |
| $C_{p,m}$ [J K$^{-1}$ mol$^{-1}$][24] | 75.23 | 84.67 |
| $C_{v,m}$ [J K$^{-1}$ mol$^{-1}$][24] | 74.44 | 84.42 |
| Density (25 °C)[a] [g cm$^{-3}$][19] | 0.997048 | 1.1044 |
| Temperature of maximum density [°C][19] | 4.0 | 11.2 |
| Compressibility [10$^{-10}$ Pa$^{-1}$][18] | 4.599 | 4.763 |
| Diffusion coefficient [10$^{-5}$ cm$^2$ s$^{-1}$][25] | 2.272 | 2.109 |
| Polarizability of vapor near 100 °C [cm$^3$ mol$^{-1}$][9] | 58.5 | 61.7 |

[a] The measurements for $H_2O$ were done at 1 atm, for $D_2O$ at 1 bar.

However, other proteins are less stable in $D_2O$ than in light water.[32,33] Also, the phase behaviour of solutes is different in $D_2O$. For instance, the critical micelle concentration is typically lower in $D_2O$ than in $H_2O$.[2,34,35] Also, ion solubilities, as well as solvation strengths differ,[36–39] *e.g.*, the heat of transfer for $CaCl_2$ between the waters is $\Delta H_t(H_2O - D_2O) = -5.0$ kJ mol$^{-1}$.[40]

However, little is known about the effects of changing the aqueous solvent from light water to $D_2O$ on mineralization. Lee *et al.*[41] explored thermodynamic effects of deuterium on the aqueous synthesis of inorganic materials, revealing new structural and magnetic properties of the obtained manganese and iron materials in $D_2O$. Lundager Madsen reported no significant effect of magnetic fields on calcium carbonate precipitation when using $D_2O$, in contrast to the observed effect in light water.[42] Raudino *et al.*[43] found that smaller crystals formed in $D_2O$ compared to $H_2O$ solutions in the case of alkaline earth carbonates. Furthermore, the conversion of calcite into aragonite in $D_2O$ seemed to be less favourable at high temperatures. Recently, Morris *et al.*[44] studied the kinetics of amorphous calcium carbonate (ACC) precipitation in $H_2O$ and $D_2O$, reporting very similar rates for the two aqueous solvents, suggesting that neither ion dehydration nor deprotonation of bicarbonate ions represented significant energetic barriers to the formation of ACC.

Considering the various effects of a solvent exchange from light to heavy water described above begs the question: which influences on the early stages of precipitation of calcium carbonate can be expected, in principle? In the following, we contemplate these possibilities within the frameworks of different existing nucleation theories.

## Potential effects of $D_2O$ *vs.* $H_2O$ according to classical nucleation theory (CNT)

According to CNT, as schematically illustrated in Fig. 1 (top), the nucleation rate $J$ can be expressed as:[46]

$$J = L \cdot \exp(-E_A/kT) \cdot \exp(-\Delta g_c/kT) \quad (1)$$

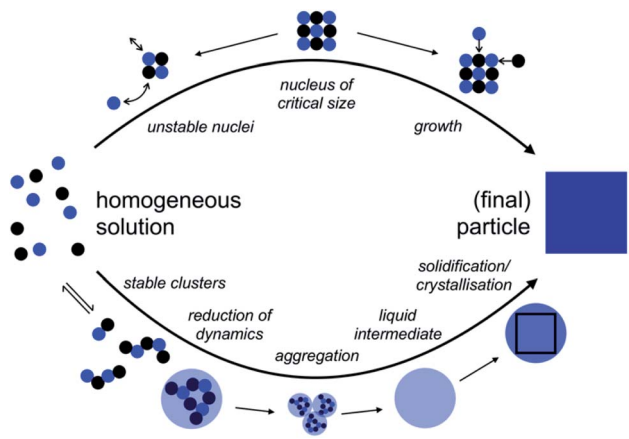


Fig. 1 Comparison of the pathways from homogeneous solution to crystals according to the notions of classical nucleation theory (CNT, top) and the pre-nucleation cluster (PNC) pathway (bottom). For explanation see the text; adopted from ref. 45.

 

where the pre-factor $L$ can be derived from the shape and material-dependent bulk properties of the nuclei. The first exponent represents the so-called "kinetic barrier" characterized by the activation energy $E_A$ (Boltzmann constant $k$, absolute temperature $T$), which is, however, probably negligible and difficult to assess *a priori* (also see below). The second exponent gives rise to the so-called "thermodynamic barrier" to nucleation characterized by the standard free energy associated with the formation of the critical nucleus, $\Delta g_c = B \cdot \alpha^3/\sigma^2$. Here, $B$ is a constant that depends on the nucleus shape and density.[46] According to CNT, $\Delta g_c$ is proportional to the cube of the interfacial free energy of the nuclei, $\alpha$, which can be obtained from the macroscopically accessible interfacial tension (capillary assumption). Also, $\Delta g_c$ is inversely proportional to the square of supersaturation $\sigma$ given by:

$$\sigma = kT \cdot \ln(\mathrm{IAP}/K_{sp}) \quad (2)$$

where IAP is the actual ion activity product (in the supersaturated, metastable solution) according to the composition of the nascent mineral phase, and $K_{sp}$ is its solubility constant.

The above considerations allow us to qualitatively analyze potential effects of the solvent change on classical nucleation behaviour. A change to heavy water is rather unlikely to affect the pre-factor, $L$, as this parameter is mainly associated with mineral bulk properties and nucleus shape. Regarding the kinetic barrier, in the case of calcium carbonate, computer simulations indeed suggested that no significant activation energies, *e.g.*, due to de-hydration of the ions, exist,[47] a notion that recent experiments seem to corroborate.[44] This then leaves the thermodynamic barrier, and it is indeed conceivable that the change of the aqueous solvent alters the surface free energy and/or the solubility constant, $K_{sp}$. As the latter enters the quantitative expressions in a logarithm (eqn (2)) that then enters the rate expression in the denominator of an exponent (eqn (1)), any potential effects of the solvent change on the interfacial free energy are expected to dominate, as this parameter is cubed and then enters the exponent for calculating the nucleation rate $J$.

The surface tension of $D_2O$ is slightly less than that of $H_2O$,[48] which is attributed to the somehow larger molecular volume and, thus, a somewhat larger separation of the dipoles in heavy water, reducing the mutual attraction between the dipoles within the bulk of the solvent. In the absence of data on interfacial tensions between calcium carbonate and heavy water, it can thus be speculated that the solvent change to heavy water would also somewhat reduce the interfacial free energies of the different polymorphs and forms, potentially by increments that are similar in magnitude. Since the interfacial free energy is cubed for the calculation of $\Delta g_c$ at a given supersaturation, and then enters the exponent for estimating the nucleation rate, corresponding effects could become large even for small changes in interfacial free energy, but would promote rather than inhibit "classical nucleation" of calcium carbonate in $D_2O$, with respect to the scenario in $H_2O$.

## Potential effects of $D_2O$ *vs.* $H_2O$ according to the pre-nucleation cluster (PNC) pathway

The so-called PNC pathway (Fig. 1, bottom) provides an alternative perspective on the mechanisms underlying the early stages of mineralization.[45,49,50] Here, thermodynamically stable solute clusters (*i.e.*, standard free energy of formation, $\Delta G^0$

< 0) form initially, independent of supersaturation. Their structural form is called a 'dynamically-ordered liquid-like oxyanion polymer' (DOLLOP).[47] A change towards higher coordination numbers than in the initially chain-like DOLLOPs in larger PNCs was suggested to significantly reduce the PNC dynamics and thereby lead to phase separation.[49,51] Indeed, the PNC size distribution depends on the actual IAP in solution, and a recently introduced quantitative framework allows predicting the specific IAPs, at which PNCs can and must transform into dense liquid calcium carbonate (nano)droplets, that is, of the corresponding liquid–liquid binodal and spinodal limits, respectively.[52] Input parameters of the experimentally verified model are, essentially, the ion association constant, $K_{cluster}$, and the solubilities of the different polymorphs, $K_{sp,polym.}$, accounting for the experimentally observed phenomenon of amorphous polymorphism in ACCs[53–55] in the binodal limit, given by the corresponding $IAP_{binodal}$:[52]

$$IAP_{binodal} = A_{polym.} \cdot K_{sp,polym.} \cdot \ln K_{cluster} \quad (3)$$

The unit-less constant $A$ was determined to be $A_{vaterite} = \sim 0.4$, $A_{aragonite} = \sim 1.0$ and $A_{calcite} = \sim 1.3$.[52] The predicted spinodal limit, $IAP_{spinodal}$, on the other hand, is given by:[52]

$$IAP_{spinodal} = 1/(K_{cluster})^2 \quad (4)$$

$IAP_{spinodal}$ agrees with the commonly accepted value of the solubility of (disordered) ACC[56] that is typically precipitated from high levels of supersaturation. Indeed, according to the PNC pathway, the as-formed liquid intermediates dehydrate towards the formation of solid ACC, as observed *in situ* recently,[57,58] thus transferring structural characteristics from the PNCs, over the liquid intermediates, to the initial amorphous solids. The solid ACCs later transform into crystals, at which stage different mechanisms may operate.[59,60]

Water plays an important role in the non-classical nucleation of calcium carbonate.[54,61,62] For instance, the entropic contribution to the overall free energy change due to the release of hydration waters from ion hydration shells during ion association drives the formation of PNCs,[63] and it is thus conceivable that the change from $H_2O$ to $D_2O$ might affect the ion association constant. For instance, since $D_2O$ is more ordered than $H_2O$ (*cf.* above), the entropic gain upon releasing hydration waters to a more ordered environment during ion association might be somewhat reduced in heavy water, which would render PNCs in $D_2O$ less stable than in $H_2O$. Since the solubilities of the different polymorphs and forms might be affected too, within the framework of the quantitative PNC model,[52] this would then shift the binodal and spinodal limits, eqn (3) and (4). With it, the critical point and the whole liquid–liquid coexistence region would be shifted, potentially giving rise even to the formation of distinct, potentially new proto-structures in ACC. In turn, new crystal polymorphs might become accessible. A changed locus of the miscibility gap would in any case alter the kinetics of liquid–liquid demixing from specific levels of supersaturation, opening up reaction channels for alternative pathways. For instance, in $D_2O$, calcium carbonate might behave more 'classically'. In our opinion, virtually anything is possible.

However, very little is known about the effects of changing the solvent from light to heavy water on calcium carbonate mineralization. Since strong effects are

possible, which promise to shed new light on the nucleation mechanisms both from a kinetic and thermodynamic perspective, we studied the early stages of calcium carbonate formation in light and heavy water, and mixtures of light and heavy water, computationally and experimentally.

## Results and discussion

### Computer simulations of PNCs in light *vs.* heavy water

The development of a flexible heavy water model and its properties are described in the Experimental section on the computational methods (ESI, Experimental section and Fig. S1, S2, Tables S1 and S2†). In brief, the parameterization by scaling the charges of the flexible water model SPC/fw led to a good $D_2O$ model (SPC/HW/fw) that correctly represents the structure of heavy water and that can be combined with the $CaCO_3$ model of Raiteri *et al.*[64]

The formation of PNCs in $D_2O$ and $H_2O$ was simulated utilizing a cubic simulation box with a side length of 55 Å, containing 10 $Ca^{2+}$- and 10 $CO_3^{2-}$-ions. The resulting concentration was 0.1 M with respect to $Ca^{2+}$-ions. 20 replicas with randomized ion positions were simulated per solvent. During the course of these simulations, clusters emerged and disappeared. These clusters were further analysed to search for differences in structure and kinetics between light and heavy water.

**Cluster size distribution.** The ions in solution were clustered with a cut-off distance of 3.6 Å, see the ESI for details.† The size distribution of the different clusters was calculated by counting the number of ions inside a cluster yielding distributions shown in Fig. 2. The change of solvent from $H_2O$ to $D_2O$ shifts the cluster size distribution to smaller structures with fewer ions.

In addition, only half so many clusters containing more than two ions, were found in $D_2O$ with respect to $H_2O$. We thus visualized the internal structure of ion aggregates by creating 2D histograms of angle–distance combinations within the clusters. Here, we looked at all ion pairs within a cut-off distance of 4.0 Å. Then we

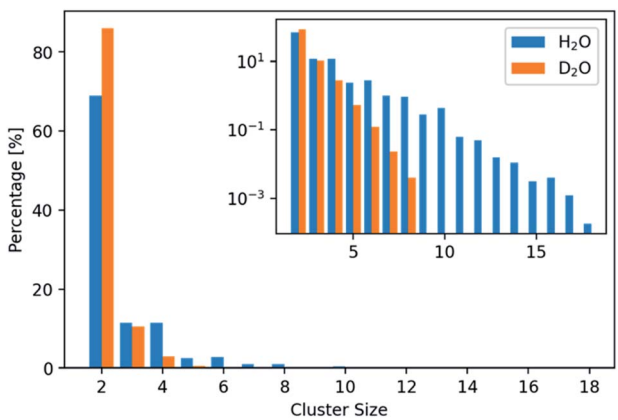


Fig. 2 Distribution of the number of ions per found cluster in light and heavy water. The distributions are normalized based on the total number of clusters found in the respective solvent. Two times more clusters (consisting of $N$(ions) > 2) were found in $H_2O$ compared to $D_2O$.

measured the distance and angle of a third ion within 8.0 Å and binned the values in histograms. The resulting histograms (Fig. S3 and S4†) show that the overall features stay the same. However, the features, especially at large angles, are less pronounced in $D_2O$. This agrees with the observation of shorter and more compact clusters in $D_2O$ and indicates that the structure of the clusters differs between the two aqueous solvents.

**Lifetime of the clusters.** The lifetime of different clusters was calculated to evaluate the kinetic stability of these species. The time while the cluster consists of three or more ions is thereby considered the lifetime of a cluster. The solvent change to $D_2O$ leads to a reduction of the lifetime of pre-nucleation clusters (Fig. 3) along with a reduction of their total number (Fig. 2). Hence, $D_2O$ reduces both their kinetic and thermodynamic stabilities with respect to the scenario in light water.

**Discussion.** The computational results show that a change from $H_2O$ to $D_2O$ leads to smaller, more compact PNCs which also occur less often and with shorter lifetimes than in light water. The potential cause of these changes remains unclear and has to be evaluated further. To this end, we first calculated the potential of mean force (PMF) between calcium and carbonate ions in the different aqueous solvents (Fig. 4). Again, it is obvious that ion association is weaker in $D_2O$ than in $H_2O$, while the general features of the PMF stay the same. The resulting differences may partially be explained by the higher dipole moment of $D_2O$, leading to a higher dielectric constant, and, with it, to a lower resulting electrostatic force between ions due to screening. In order to study this effect further, the ion association constant was calculated using the PMF, following the approach used by Raiteri *et al.*[64] The ratio of the association constants in the distinct aqueous solvents should be rather robust to errors that might occur when analysing the PMF. Indeed, the association constant is 6 times higher in $H_2O$ than in $D_2O$ (Fig. S5†), explaining why fewer and smaller clusters are observed in heavy water than in light water.

The difference in mass between the two aqueous solvents is often considered to be the only difference, while changes of internal structure and polarizability are

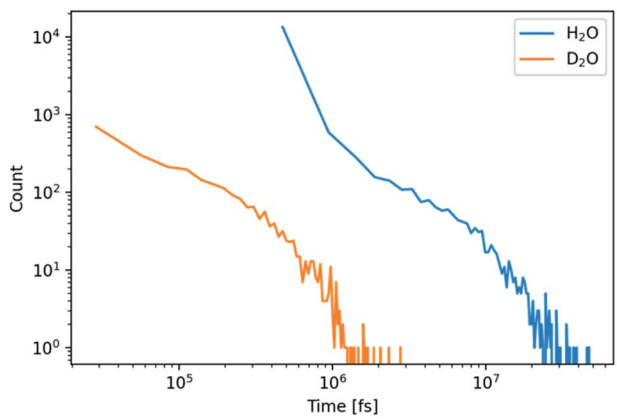


Fig. 3 Histogram of the lifetime of $CaCO_3$ clusters containing more than 3 ions for simulations in $H_2O$ and $D_2O$ as indicated.

 

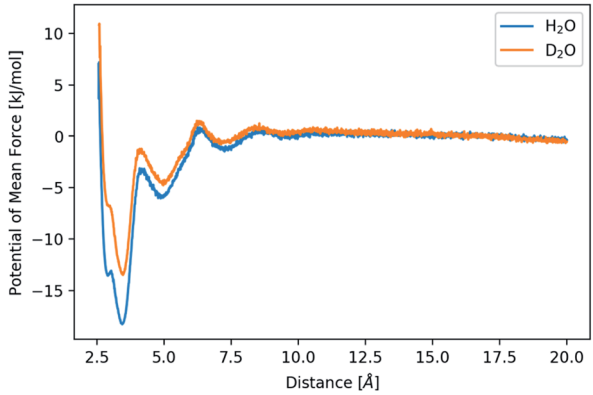


Fig. 4 Potential of mean force for the distance between calcium and carbonate ions in $H_2O$ and $D_2O$ as indicated.

often neglected. So as to investigate the over-simplified assumption further, an $H_2O$ model with masses of $D_2O$ was simulated. The corresponding 2D histogram of the radius of gyration *vs.* cluster size (Fig. S6†) reveals no structural changes between the clusters in $H_2O$ and in $H_2O$ with increased masses, that is, in "pseudo-$D_2O$". Also, the distribution of cluster sizes persists after the mass change (Fig. S7†). Only the lifetime of these clusters in "pseudo-$D_2O$" decreases (Fig. S8†). Thus, these simulations of "pseudo-$D_2O$" reveal that the above-described change in behaviour arises from the change of the charge distribution within the solvent rather than from the mass difference of the two aqueous solvents.

### Titration assays of calcium carbonate formation

So as to elucidate the effects of a solvent change from light to heavy water experimentally, we performed titration experiments in different mixtures of the two aqueous solvents, as well as in pure $H_2O$ and 99% $D_2O$. In brief, dilute calcium solution was added into dilute carbonate buffers, while the pH was maintained at a constant value by automatic counter-titration with dilute sodium hydroxide solution. The specific $H_2O/D_2O$ ratio (v/v) in these solutions was the same, and adjusted to 100/0, 87.5/12.5, 75/25, 62.5/37.5, 50/50, 25/75 and 0/99 in separate repetitions. The pH of the respective mixtures was thereby adjusted to a value that corresponds to the same carbonate/bicarbonate ratio in the buffer in pure $H_2O$ at pH 9.00 (for details see ESI,† Experimental section). This is the equivalent pH of these aqueous mixtures enabling direct comparison of the titration profiles.

Initially, the calcium carbonate ion activity product (IAP) increases linearly until it drops to a plateau during the course of the titration (Fig. 5). Due to the very slow titration, the linear parts of the curves represent equilibrated (meta)stable states.[65] The slope of the pre-nucleation part (*i.e.*, before the steep drop of the IAP) thus correlates with the equilibrium constant for ion association yielding PNCs, whereas a flatter slope points towards a larger equilibrium constant, *i.e.*, more stable ion associates. On the other hand, the post-nucleation plateau value (*i.e.*,

after the steep drop of the IAP) represents the solubility of the initially precipitated phase. Note that the most soluble phase determines these solubility measurements, that is, ripening towards more stable (less soluble) forms is only visible in the titration profiles once the more soluble one has completely

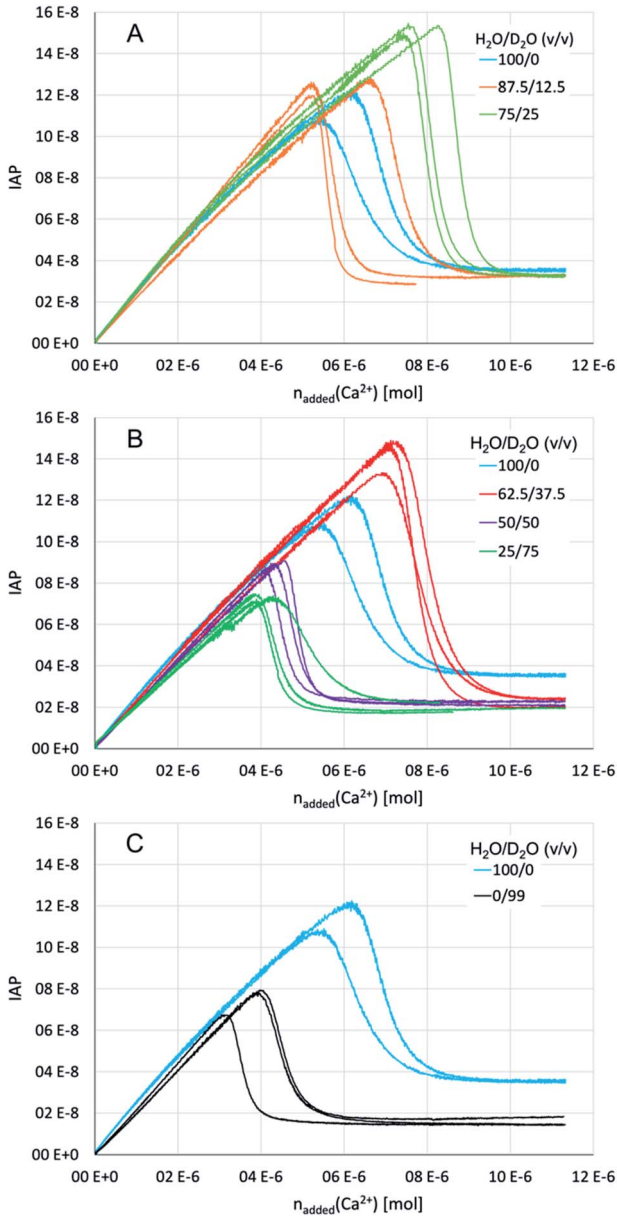


Fig. 5 Titration profiles for different $H_2O$ and $D_2O$ mixtures at an equivalent pH of 9.00 in pure water as indicated for (A) low heavy water contents; (B) high heavy water contents; (C) pure light *vs.* 99% heavy water. The data for pure light water is identical in panels (A), (B), and (C) so as to facilitate comparison. Individual repetitions are shown in the same respective colours, so as to illustrate reproducibility.

 

dissolved. In pure water, the IAP of $\sim 3.5 \times 10^{-8}$ corresponds to the solubility of proto-calcite amorphous calcium carbonate (pc-ACC).[53,65] At the same time, this IAP corresponds to the liquid–liquid binodal limit, $IAP_{binodal} = \sim 3.5 \times 10^{-8}$, as demonstrated by THz spectroscopy,[66] which can be quantitatively predicted based on eqn (3).[52] Indeed, the IAP development upon exceeding the binodal limit represents liquid–liquid coexistence, and strong evidence suggests that the initially formed solid pc-ACC is formed *via* dehydration of the dense liquid precursors.[52] In this sense, the delay between exceeding the binodal limit and the steep drop in IAP is associated with the kinetics of dehydration of phase-separated dense liquid rather than nucleation kinetics *per se*. In any case, it is obvious that the change from light to heavy water influences (i) the pre-nucleation slope, (ii) the point of nucleation, and (iii) the solubility of the initially precipitated phase. In the following, we discuss these observations individually.

**Effects on pre-nucleation slope.** At low $D_2O$ contents ($H_2O/D_2O$ ratios of 87.5/12.5 and 75/25, Fig. 5A), the pre-nucleation slope seems to be largely unaffected by the presence of heavy water, especially concerning the initial development before reaching the liquid–liquid binodal limit (the one for pure $H_2O$, *i.e.*, $\sim 3.5 \times 10^{-8}$). If anything, above $IAP_{binodal}$, the IAP pre-nucleation development in pure light water bends down earlier than in the solvent mixtures with low heavy water contents. This might indicate that dehydration of phase-separated dense liquid (nano)droplets is, by comparison, kinetically weakly inhibited (see below) in the presence of low amounts of heavy water.

On the other hand, there seem to be no distinct effects of the low heavy water contents on the ion association thermodynamics. However, with increasing heavy water contents ($H_2O/D_2O$ ratios of 50/50 and 25/75, Fig. 5B), the pre-nucleation slope becomes noticeably flatter, with a minimum at 75% $D_2O$. In terms of standard free energy of ion pair formation, the ion associates are by *ca.* 2 kJ mol$^{-1}$ more stable in a mixture of $H_2O/D_2O$ of 25/75 than in pure light water. However, the trend appears to be reversed in 99% heavy water (Fig. 5C), where the pre-nucleation slope is essentially parallel to the one observed in pure light water, even though the IAP development in 99% heavy water is curved downwards in the very early stage of the experiment (*i.e.*, before the IAP values are reached that are established in the post-nucleation plateau), as opposed to pure light water. In this sense, the experimental data on ion association seems to contradict our results from computer simulations; if anything, ion associates are somewhat more stable in the presence of heavy water.

**Effects on the point of nucleation.** Above 12.5% $D_2O$, the steep drop in IAP is shifted to higher added amounts of calcium ions (and higher maximal IAPs) in comparison to pure light water as the reference (Fig. 5A), indicating that the presence of low amounts of $D_2O$ in the solvent mixtures inhibits dehydration processes of the dense liquid precursors. A similar effect is observed in 37.5% $D_2O$ (Fig. 5B). However, when an effect of the presence of heavy water on the stability of ion associates becomes noticeable in the 50/50 mixture (see above), the drop in the IAP occurs earlier, now indicating that dehydration of dense liquid precursors is facilitated at even higher heavy water contents—if liquid–liquid separation still occurs in these systems. Notably, this behaviour does not directly correlate with the development of the post-nucleation solubility thresholds (see below), as a distinctly more stable phase is formed initially already in 37.5% $D_2O$, where nucleation is still inhibited rather than promoted.

**Effects on solubilities of initially precipitated phases.** In the presence of low amounts of heavy water ($H_2O/D_2O$ ratios of 87.5/12.5 and 75/25, Fig. 5A), the solubility of the initially precipitated phase decreases slightly and is now on the order of $\sim 3.3 \times 10^{-8}$. While the difference in solubility compared to the situation in pure light water is small, it is on the order of the difference of the solubilities of pc-ACC and proto-vaterite-ACC (pv-ACC),[53,65] and thus seems to be significant. Upon increasing the $D_2O$ content from 25% to 37.5%, the solubility of the initially precipitated phase decreases further, and is then on the order of $1.7 \times 10^{-8}$ to $2.3 \times 10^{-8}$, which is slightly above the solubility of vaterite in pure water at 25 °C ($1.2 \times 10^{-8}$).[56] Considering the reproducibility of the measurements in different mixtures, it seems that there is no obvious trend, but rather a switch to a different behaviour. This could be due to a shift of the liquid–liquid binodal limit that is caused by a change in the solubility of the different polymorphs or the constant $A$ (eqn (3)). Indeed, according to the theory (eqn (3)), a change in solubilities or $A$ would have a significantly stronger effect on the locus of the liquid–liquid binodal limit than altered ion association thermodynamics. On the other hand, the dehydration and crystallization kinetics might be significantly faster in the presence of higher amounts of heavy water, too, leading to the accelerated formation of vaterite, thereby potentially missing solid ACC intermediates in the development of the IAP. Third, liquid–liquid separation as a precursor to ACC may not occur in the solvent mixtures at higher heavy water contents, and nucleation of vaterite might occur directly, *i.e.*, "classically". In order to elucidate these possibilities further, we attempted to quench the amorphous intermediates in an excess of ethanol, as established for the isolation of proto-structured ACCs in pure light water.[53,54] In $H_2O$, ethanol serves as a drying agent for the liquid–liquid separated dense calcium carbonate droplets, but at high contents of $D_2O$, unfortunately, the solubilities of sodium bi/carbonate become an issue for this isolation procedure, and we largely obtained crystalline sodium bi/carbonate in ethanol quenches in the presence of heavy water—with additional reflexes (Cu-K$\alpha$) at $\sim 24°$, $\sim 27°$ and $\sim 33°$ $2\theta$, which we could not assign to any compound that is in principle accessible in this system (Fig. S9†).

### ATR-FTIR kinetic investigations

The titration experiments suggest that at relatively low levels of supersaturation (*i.e.*, close to the binodal limit), low amounts of heavy water may inhibit the dehydration kinetics of liquid–liquid separated states towards the formation of solid ACCs, while even higher amounts of heavy water may, in turn, accelerate precipitation and crystallisation in this region of the phase diagram—if the liquid–liquid miscibility gap still exists in $D_2O$ containing solutions. In order to explore the precipitation kinetics from the putative spinodal regime of the phase diagram, *i.e.*, at high levels of initial supersaturation, we implemented stopped-flow mixing experiments monitored over time by ATR-FTIR (see the ESI for experimental details†). Calcium chloride (0.2 M) and sodium carbonate (0.2 M) solutions were prepared in different $H_2O/D_2O$ mixtures (100/0; 87.5/12.5; 75/25; 50/50 and 0/100) and corresponding normalised time transients after mixing were extracted at 869 $cm^{-1}$, corresponding to the minimum of the second derivative of the $\nu_2$ carbonate vibrational band. These concentrations—at least for the pure $H_2O$ sample—lead to liquid–liquid demixing from the spinodal regime

of the aqueous calcium carbonate phase diagram.[52] However, as per the theory (eqn (4)), the altered ion association thermodynamics would shift the spinodal regime to lower IAPs for intermediate heavy water contents, due to the somewhat higher ion association constant.

Indeed, the time transients (Fig. 6A) strongly differ for the different aqueous mixtures. In pure light water, we observe a steep initial increase, which gradually flattens, kinks, and then develops into a plateau. In an $H_2O/D_2O$ mixture of 87.5/12.5, the initial increase is significantly flatter, and the transient does not seem to even come close to reaching a final plateau as observed in pure light water, within the observation time (note that due to the normalization to the plateau value, which is not reached in the experiment with 12.5% heavy water, the initial kinetics is probably the slowest in this mixture). However, a plateau is again

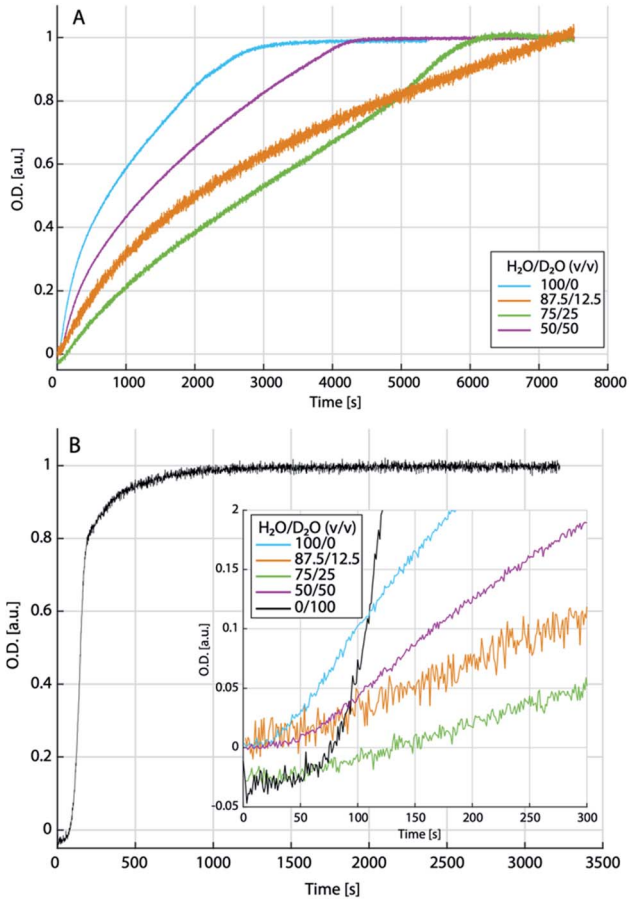


Fig. 6 Normalised transients extracted from the time development of the $\nu_2$ carbonate vibrational band upon mixing 0.2 M calcium and carbonate solutions (liquid–liquid spinodal regime for pure light water) in different mixtures of light and heavy water as indicated (A); and in essentially pure (99.9%) heavy water (B). The inset in (B) shows a zoom into the early times of the transients shown in (A), together with the transient for heavy water.

reached in the 75/25 mixture within the observation time. In the 50/50 mixture, the kinetics are then again closest to the situation in pure water. Also qualitatively, the kinetics of calcium carbonate precipitation in the 50/50 mixture is similar to the pure light water system, while at low heavy water content (75/25), the transient exhibits rather distinct features. In almost pure heavy water (99.9%; Fig. 6B), on the other hand, the transient looks again completely distinct. Initially, there is a rather flat linear increase for *ca.* 50–70 s (inset of Fig. 6B) before the transient directly develops into a plateau value with the steepest increase and thus, fastest kinetics observed in all solvent mixtures. In the other solvent mixtures (see inset of Fig. 6B), but not pure light water, we find a similarly flat initial slope, however, the very steep increase as in 99.9% heavy water does not occur.

Only in the 50/50 mixture, there is a notable upwards kink after *ca.* 50 s, which then gradually levels off after *ca.* 150 s. In pure light water, a less steep increase than in heavy water occurs after *ca.* 25 s and we interpret this as the time required for a sufficient amount of calcium carbonate to sediment on the ATR crystal, rather than an induction time. Indeed, a similar "deadtime" is observed in all other transients. However, the extended, flat, initial linear regime in presence of heavy water could be interpreted as the presence of an induction time, which would then provide evidence that we did not probe the spinodal regime in presence of pure heavy water. Unfortunately, due to heavily convoluted carbonate and aqueous solvent bands, the single spectra (data not shown) cannot be evaluated towards an assignment of different calcium carbonate forms to the different kinetic stages in any solvent mixture, at this time.

### Simulations of residence times of water molecules and water exchange

Our kinetic analyses provide evidence for distinct effects of the solvent mixtures in the binodal as well as putative spinodal regimes. In order to explore these observations further, computationally, we studied the residence time of water in the first solvation shell of the ions. The average time that a water molecule stays within the solvation shell was calculated utilizing a self-developed method by bookkeeping the ions and *via* a time correlation function (see ESI,† Experimental section, for details). The water exchange for calcium ions in heavy water is around two times slower than in light water (Table S4†). The errors observed for both methods show that the residence times of water vary substantially with a maximum value of 1.8 ns for calcium ions in light and 4.8 ns in heavy water, while the average times are on the order of experimentally determined values. Notably, previous calculations of the water residence time for calcium ions in light water with MD simulations yielded a large range of values, depending on the used force field,[67] or more precisely, on the size of ions and the water models. An influence of the box size was also found, with a smaller box leading to shorter residence times.[68] The difference between water and heavy water may occur due to the changes in mass and charge between the models. However, the change in charge from SPC to TIP3P is around +1.7%, while the change from SPC/fw to SPC/fw/HW is around +2.7%. In the case of SPC *vs.* TIP3P (GROMOS96 *vs.* GROMOS87), the residence time decreases by 10%. In the case of water to heavy water, it increases by over 100%. The increase in residence time for $D_2O$ seems to

depend on the change in mass and maybe slightly stronger ion–water interactions.

Moreover, in kinetic measurements, the mixing behaviour of the two aqueous solvents might play additional roles, *i.e.*, the dynamics of light water/heavy water exchange of the ions and potential memory effects. Mixtures of $H_2O$ and $D_2O$ were simulated while the issue of the formation or presence of HDO molecules was not covered. Negative controls of pure $H_2O/D_2O$ mixtures without ions showed a rapid mixing of both previously separated phases without any form of aggregation present. The interactions of the ions with the mixed solvents were tested with two setups. On one hand, an ion was simulated in one of the solvents. Then, the ion and a sphere of water, consisting of the first and second solvation shell ($Ca^{2+}$: 5.4 Å; $CO_3^{2-}$: 6.2 Å), was cut out and placed in a box of the other solvent. On the other hand, the box was split into two equal compartments and the ion placed in either one of them. After an equilibration with position restrains, the coordination number of light and heavy water in the first shell was monitored, as shown in Fig. 7. At first glance, the behaviours of the systems seem similar, independent of the placement in $H_2O$ or $D_2O$. Yet, there are minor differences between the two solvents. In the first setup, with a calcium ion in a sphere of $H_2O$ placed in $D_2O$, the $H_2O$ is completely dissolved in $D_2O$ and the ion is exclusively surrounded by $D_2O$ molecules during the second half of the simulation, from 5 ns after mixing onwards. When a sphere of $D_2O$ is placed in $H_2O$, we observe a similar effect. However, at least one $D_2O$ molecule detaches and reattaches repeatedly during the whole course of the simulation. In the case of the second setup, with an equal amount of both solvents present, there are on average 1.7 more $D_2O$ molecules present around the ion than $H_2O$ molecules.

The fluctuation of $H_2O$ and $D_2O$ around the ion is smaller in the case where the ion is placed directly in $D_2O$. Both setups show that the calcium ion is more attracted to $D_2O$ and is thus more influenced by it in mixtures. The second observation indicates that $D_2O$ could form a stable solvation shell upon time,

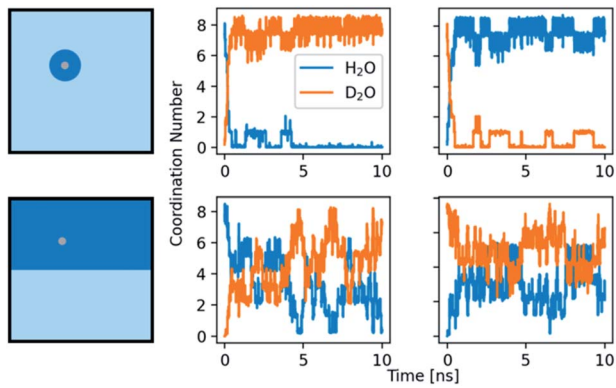


Fig. 7 Coordination number of $H_2O$ and $D_2O$ around a calcium ion. The rows show the results for two different setups. Top row: the ion with its first and second solvation shell is placed in the opposite solvent. Bottom row: the box is split into two compartments containing $H_2O$ and $D_2O$ and the ion is placed in one of them. Left: schemes of the initial setups. Middle: calcium ion initially surrounded by $H_2O$. Right: calcium ion initially surrounded by $D_2O$.

maybe with stable, chelating motifs in it. The light water exchange with this solvation shell appears to be slower. The formation of a more stable solvation shell after some induction time is a known problem in MD simulation of magnesium ions, especially in conjunction with RNA.[69–72] The better solubility of some ions and small molecules in $D_2O$ is also known, assumed to be caused by its different compressibility and hydrophobicity.[29]

# Discussion

We observed various, distinct effects of the aqueous solvents, $D_2O$ *vs.* $H_2O$, on the early stages of calcium carbonate formation, both computationally and experimentally. In MD simulations of ion association in $D_2O$, to which end we developed a suitable force field that is also presented herein, the number of calcium carbonate clusters (PNCs) was reduced by a factor of two when compared to the situation in light water. Furthermore, the clusters in $D_2O$ were smaller and more compact than the ones found in $H_2O$, and also shorter lived. This could indicate that nucleation processes in $D_2O$ might be "more classical" as the role of PNCs would be reduced, and the cluster distribution shifted more towards single ions or ion pairs—as reflected by a *ca.* 6 times smaller ion association constant in $D_2O$ than in $H_2O$. Simulations of a "pseudo-$D_2O$", *i.e.*, where only the mass of light water was altered, showed that rather than mass differences, the distinct charge distribution within the aqueous solvents is the key to the different behaviours. The residence time of water molecules on calcium ions is increased by a factor of 2.2–2.5 in $D_2O$, and there seems to be a somewhat higher attraction of calcium ions to $D_2O$ molecules, indicating that the ion interactions are probably influenced already at low $D_2O$ concentrations in $H_2O$ solution. Furthermore, indications were found that the behaviour of the solvent mixtures was determined by its initial condition—*i.e.*, whether a calcium ion was dissolved in $D_2O$ or $H_2O$ prior to mixing. All of the computationally observed differences between the behaviours of calcium carbonate in $D_2O$ and $H_2O$ are eventually due to changes in water properties, ion–water interactions and cluster formation, which could even lead to different calcium carbonate structures and formation pathways.

Indeed, experimentally, we observed distinct effects of the solvent exchange as well, however, the influence on ion association has the opposite trend when compared to the computer simulations (*i.e.*, ion associates become somewhat more stable in the presence of heavy water in experiments), and the effect is only on the order of thermal energy in terms of standard free energies. Also, with increasing $D_2O$ contents, there is no clear trend, and the behaviour somehow reverses again when approaching pure heavy water, in the binodal regime of calcium carbonate formation. This could indicate that in purest heavy water (note that for cost reasons, we employed 99% heavy water in the titration assays, but did use 99.9% heavy water in the ATR-IR-based kinetic analyses), there might actually be a (slight) decrease in stability of ion associates also in experiments. At low heavy water contents in the binodal regime of calcium carbonate formation, dehydration processes of dense liquids towards the formation of solid ACC seem to be weakly inhibited, which is in line with the computer simulations and the residence times of the water molecules on the ions. It is difficult to find information on the kinetics of the exchange of H and D between $D_2O$ and $H_2O$ in the literature. Mammoli *et al.*[73] assessed the lifetime of proton exchange to be on the

order of ~1 ms in pure water. If this holds true also for the D nucleus, at least for the order of magnitude, corresponding exchanges should be no issue at all with regards to our ATR-FTIR kinetic analysis (where timescales of seconds are discussed). Also, the exchange of H/D should be slow enough so that the computational analysis of the lifetimes of water around calcium-ions are not affected, because the interconversion should be slower than ion–water exchange.

The complex dependence of the calcium carbonate formation pathway on different light/heavy water mixtures is also reflected in kinetic measurements of calcium carbonate formation from high initial levels of supersaturation. While in pure light water, we probed the spinodal regime towards calcium carbonate liquid–liquid demixing, in the presence of heavy water, we observed initial rather flat slopes that might point towards the presence of an induction time for calcium carbonate formation at the same initial IAPs. This suggests that in the presence of heavy water, we might still have probed the kinetics of precipitation of calcium carbonate in the binodal regime. At this point, it remains unclear whether the locus of the liquid–liquid miscibility gap was altered in unpredictable ways, if it even still exists, or whether indeed, calcium carbonate nucleation proceeded "more classically". The latter might explain the observation of Lundager Madsen[42] that there was no effect of magnetic fields on calcium carbonate formation in heavy water (as opposed to light water), since Coey's theory[74] on the effects of magnetic fields on scaling relies on the role of PNCs. The found influence of the solvent and solvent mixture on the point of nucleation of the initial solid is interesting in this regard, and low amounts of heavy water in $H_2O$ seem to inhibit the dehydration processes towards formation of solid ACC. The reverse observed behaviour at higher heavy water contents (*i.e.*, promoting nucleation) might indeed reflect that a distinct pathway is populated under these conditions. Thus, above *ca.* 40% $D_2O$, vaterite may form directly rather than *via* liquid–liquid separation and solid ACC. After all, this could occur even if liquid–liquid separation still happens in these solvent mixtures, *i.e.*, when the kinetics of dehydration of "non-classical" intermediates is reduced and the classical rate of direct nucleation is increased (potentially, due to lower interfacial free energies of crystals in heavy water, *cf.* the introductory section). This could be the case to an extent that the classical pathway becomes significantly more populated than the "non-classical" one *via* PNCs, once heavy water contents are high enough, *i.e.*, above *ca.* 40% heavy water. However, the kinetics of ACC formation might, on the other hand, be accelerated in these mixtures, so they are not observable in our experiments, and unfortunately, we were not able to isolate the intermediate states due to solubility issues of sodium carbonates in these aqueous solvent mixtures. Notably, it cannot be excluded that new, distinct forms of ACC or even crystalline calcium carbonate become accessible—for which there are at least some indications (Fig. S9†).

When comparing the results from experiment and computations, it has to be kept in mind that the latter did not account for HDO molecules, which might actually be an important species for explaining the experimentally observed behaviour, especially at low heavy water contents. Note that in these mixtures, no significant fractions of $D_2O$ are expected to be present, but they would rather be mixtures of mostly $H_2O$ and HDO. The changed trends observed in the titration assays may then correlate with the onset of the presence of significant $D_2O$ contents within $H_2O$/HDO mixtures. Also, the unclear trends upon changing the

compositions of the mixtures in a systematic fashion indicate that there might be a complex, underlying phase behaviour of the water systems, which seems to be rather complicated already in pure light water alone,[75] and which might in turn distinctly affect the calcium carbonate formation pathway.

## Conclusions

In our opinion, further studies of the differences in the behaviours of aqueous calcium carbonate systems in $D_2O$ and $H_2O$, and mixtures thereof, open up unprecedented possibilities for obtaining a better understanding of nucleation and crystallisation mechanisms in the future, and we believe that also the behaviour of other mineral systems in such different aqueous systems should be explored. However, our study provides a warning towards usage of different experimental data, too. Many experiments use $D_2O$ as substitute for $H_2O$, for example, so as to get rid of unwanted spectral backgrounds, or for other reasons (also see the introduction section). However, in terms of mineralisation, our data unambiguously demonstrates that the pathway can be considerably altered, depending on the specific solvent (mixture). Notably, experimental data from heavy water systems are sometimes used for the creation of $H_2O$-based (!) models in computer simulations, where the original solvent may not even be mentioned in citations, and mechanisms are then erroneously treated to arise from light water properties. Thus, considering the distinct differences between the waters might even reconcile previous, seemingly contradicting results.

## Author contributions

Conceptualization: DG, KH, CP; data curation: JTA, MK, CP; formal analysis: JTA, MK, DG; funding acquisition: CP, KH, DG; investigation: JTA, MK; methodology: JTA, MK, CP, KH, DG; project administration: CP, KH, DG; resources: CP, KH, DG; software: JTA, MK, CP; supervision: CP, KH, DG; validation: JTA, MK; visualization: JTA, MK, DG; writing – original draft: MK, DG; writing – review & editing: JTA, MK, CP, KH, DG.

## Conflicts of interest

There are no conflicts to declare.

## Acknowledgements

We gratefully acknowledge funding by the German Research Foundation (DFG) through SFB1214 (projects A02 and A04). The authors acknowledge support by the state of Baden-Württemberg through bwHPC and the German Research Foundation (DFG) through grant INST 35/1134-1 FUGG.

## Notes and references

1 J. J. Katz, *Am. Sci.*, 1960, **48**, 544–580.
2 G. C. Kresheck, H. Schneider and H. A. Scheraga, *J. Phys. Chem.*, 1965, **69**, 3132–3144.

 

3 S. Scheiner and M. Čuma, *J. Am. Chem. Soc.*, 1996, **118**, 1511–1521.
4 G. Zuber, S. J. Prestrelski and K. Benedek, *Anal. Biochem.*, 1992, **207**, 150–156.
5 K. Hauser, C. Krejtschi, R. Huang, L. Wu and T. A. Keiderling, *J. Am. Chem. Soc.*, 2008, **130**, 2984–2992.
6 M. Jawurek, J. Dröden, B. Peter, C. Glaubitz and K. Hauser, *Chem. Phys.*, 2018, **512**, 53–61.
7 A. Krüger, A. Bürkle, K. Hauser and A. Mangerich, *Nat. Commun.*, 2020, **11**, 2174.
8 H. H. Mantsch, H. Saitô and I. C. P. Smith, *Prog. Nucl. Magn. Reson. Spectrosc.*, 1977, **11**, 211–272.
9 G. Némethy and H. A. Scheraga, *J. Chem. Phys.*, 1964, **41**, 680–689.
10 T. Clark, J. Heske and T. D. Kühne, *ChemPhysChem*, 2019, **20**, 2461–2465.
11 A. Zeidler, P. S. Salmon, H. E. Fischer, J. C. Neuefeind, J. M. Simonson and T. E. Markland, *J. Phys.: Condens. Matter*, 2012, **24**, 284126.
12 R. L. Cook, F. C. D. Lucia and P. Helminger, *J. Mol. Spectrosc.*, 1974, **53**, 62–76.
13 A. K. Soper and C. J. Benmore, *Phys. Rev. Lett.*, 2008, **101**, 353.
14 J. H. Root, P. A. Egelstaff and A. Hime, *Chem. Phys.*, 1986, **109**, 437–453.
15 B. Tomberli, C. J. Benmore, P. A. Egelstaff, J. Neuefeind and V. Honkimäki, *J. Phys.: Condens. Matter*, 2000, **12**, 2597–2612.
16 R. T. Hart, C. J. Benmore, J. Neuefeind, S. Kohara, B. Tomberli and P. A. Egelstaff, *Phys. Rev. Lett.*, 2005, **94**, 047801.
17 R. A. Kuharski and P. J. Rossky, *J. Chem. Phys.*, 1985, **82**, 5164–5177.
18 M. N. Rodnikova, *J. Mol. Liq.*, 2007, **136**, 211–213.
19 *CRC Handbook of Chemistry and Physics*, ed. D. R. Lide, 89th edn, Taylor & Francis Ltd, 2019.
20 M. Chaplin, https://water.lsbu.ac.uk/water/, accessed July 2, 2020.
21 R. A. Robinson, M. Paabo and R. G. Bates, *J. Res. Natl. Bur. Stand., Sect. A*, 1969, **73A**, 299.
22 M. Ceriotti, W. Fang, P. G. Kusalik, R. H. McKenzie, A. Michaelides, M. A. Morales and T. E. Markland, *Chem. Rev.*, 2016, **116**, 7529–7550.
23 J. Curry and Z. Z. Hugus, *J. Am. Chem. Soc.*, 1944, **66**, 653–655.
24 M. Nakamura, K. Tamura and S. Murakami, *Thermochim. Acta*, 1995, **253**, 127–136.
25 D. Eisenberg and W. Kauzmann, *The Structure and Properties of Water*, Oxford University Press, 2005.
26 A. Streitwieser and H. S. Klein, *J. Am. Chem. Soc.*, 1963, **85**, 2759–2763.
27 M. M. Lopez and G. I. Makhatadze, *Biophys. Chem.*, 1998, **74**, 117–125.
28 E. Wilhelm, R. Battino and R. J. Wilcock, *Chem. Rev.*, 1977, **77**, 219–262.
29 G. Hummer, S. Garde, A. E. García and L. R. Pratt, *Chem. Phys.*, 2000, **258**, 349–370.
30 G. Graziano, *J. Chem. Phys.*, 2004, **121**, 1878–1882.
31 B. Kuhlman and D. P. Raleigh, *Protein Sci.*, 1998, **7**, 2405–2412.
32 G. I. Makhatadze, G. M. Clore and A. M. Gronenborn, *Nat. Struct. Biol.*, 1995, **2**, 852–855.
33 R. Guzzi, L. Sportelli, C. L. Rosa, D. Milardi and D. Grasso, *J. Phys. Chem. B*, 1998, **102**, 1021–1028.
34 G. C. Kresheck, *J. Am. Chem. Soc.*, 1998, **120**, 10964–10969.
35 Y. R. E. Silva and J. R. Grigera, *RSC Adv.*, 2015, **5**, 70005–70009.
36 H. S. Taylor, E. R. Caley and H. Eyring, *J. Am. Chem. Soc.*, 1933, **55**, 4334–4335.

37 E. C. Noonan, *J. Am. Chem. Soc.*, 1948, **70**, 2915–2918.
38 A. A. Sunier and J. Baumbach, *J. Chem. Eng. Data*, 1976, **21**, 335–336.
39 M. Jelińska-Kazimierczuk and J. Szydłowski, *J. Solution Chem.*, 1996, **25**, 1175–1184.
40 J. Greyson and H. Snell, *J. Phys. Chem.*, 1969, **73**, 3208–3214.
41 J. Lee, N. D. Chasteen, G. Zhao, G. C. Papaefthymiou and S. M. Gorun, *J. Am. Chem. Soc.*, 2002, **124**, 3042–3049.
42 H. E. Lundager Madsen, *J. Cryst. Growth*, 2004, **267**, 251–255.
43 M. Raudino, F. Sarri, D. Tatini, M. Ambrosi, G. D. Aloisi, B. W. Ninham, L. Dei and P. Lo Nostro, *J. Solution Chem.*, 2020, **49**, 289–305.
44 P. D. Morris, I. J. McPherson, G. N. Meloni and P. R. Unwin, *Phys. Chem. Chem. Phys.*, 2020, **22**, 22107–22115.
45 D. Gebauer, *Minerals*, 2018, **8**, 179.
46 J. J. De Yoreo and P. G. Vekilov, *Rev. Mineral. Geochem.*, 2003, **54**, 57–93.
47 R. Demichelis, P. Raiteri, J. D. Gale, D. Quigley and D. Gebauer, *Nat. Commun.*, 2011, **2**, 590.
48 G. Jones and W. A. Ray, *J. Chem. Phys.*, 1937, **5**, 505–508.
49 D. Gebauer, M. Kellermeier, J. D. Gale, L. Bergström and H. Cölfen, *Chem. Soc. Rev.*, 2014, **43**, 2348–2371.
50 D. Gebauer and S. E. Wolf, *J. Am. Chem. Soc.*, 2019, **141**, 4490–4504.
51 A. F. Wallace, L. O. Hedges, A. Fernandez-Martinez, P. Raiteri, J. D. Gale, G. A. Waychunas, S. Whitelam, J. F. Banfield and J. J. De Yoreo, *Science*, 2013, **341**, 885–889.
52 J. T. Avaro, S. L. P. Wolf, K. Hauser and D. Gebauer, *Angew. Chem., Int. Ed.*, 2020, **59**, 6155–6159.
53 D. Gebauer, P. N. Gunawidjaja, J. Y. P. Ko, Z. Bacsik, B. Aziz, L. J. Liu, Y. F. Hu, L. Bergström, C.-W. Tai, T.-K. Sham, M. Edén and N. Hedin, *Angew. Chem., Int. Ed.*, 2010, **49**, 8889–8891.
54 M. Farhadi Khouzani, D. M. Chevrier, P. Zhang, N. Hedin and D. Gebauer, *Angew. Chem., Int. Ed.*, 2016, **55**, 8117–8120.
55 J. H. E. Cartwright, A. G. Checa, J. D. Gale, D. Gebauer and C. I. Sainz-Díaz, *Angew. Chem., Int. Ed.*, 2012, **51**, 11960–11970.
56 L. Brečević and A. E. Nielsen, *J. Cryst. Growth*, 1989, **98**, 504–510.
57 D. J. Kelly, N. Clark, M. Zhou, D. Gebauer, R. V. Gorbachev and S. J. Haigh, *Adv. Mater.*, 2021, **33**, 2100668.
58 P. J. M. Smeets, A. R. Finney, W. J. E. M. Habraken, F. Nudelman, H. Friedrich, J. Laven, J. J. De Yoreo, P. M. Rodger and N. A. J. M. Sommerdijk, *Proc. Natl. Acad. Sci. U. S. A.*, 2017, **114**, E7882–E7890.
59 J. Ihli, W. C. Wong, E. H. Noel, Y.-Y. Kim, A. N. Kulak, H. K. Christenson, M. J. Duer and F. C. Meldrum, *Nat. Commun.*, 2014, **5**, 3169.
60 E. Ruiz-Agudo, C. V. Putnis and A. Putnis, *Chem. Geol.*, 2014, **383**, 132–146.
61 P. Raiteri and J. D. Gale, *J. Am. Chem. Soc.*, 2010, **132**, 17623–17634.
62 H. Du and E. Amstad, *Angew. Chem., Int. Ed.*, 2020, **59**, 1798–1816.
63 M. Kellermeier, P. Raiteri, J. K. Berg, A. Kempter, J. D. Gale and D. Gebauer, *ChemPhysChem*, 2016, **17**, 3535–3541.
64 P. Raiteri, R. Demichelis and J. D. Gale, *J. Phys. Chem. C*, 2015, **119**, 24447–24458.
65 D. Gebauer, A. Völkel and H. Cölfen, *Science*, 2008, **322**, 1819–1822.

 

66 F. Sebastiani, S. L. Wolf, B. Born, T. Q. Luong, H. Cölfen, D. Gebauer and M. Havenith, *Angew. Chem., Int. Ed.*, 2016, **56**, 490–495.
67 D. Di Tommaso and N. H. de Leeuw, *J. Phys. Chem. B*, 2008, **112**, 6965–6975.
68 J. Anwar and P. K. Boateng, *J. Am. Chem. Soc.*, 1998, **120**, 9600–9604.
69 N. M. Fischer, M. D. Polêto, J. Steuer and D. van der Spoel, *Nucleic Acids Res.*, 2018, **46**, 4872–4882.
70 O. Allnér, L. Nilsson and A. Villa, *J. Chem. Theory Comput.*, 2012, **8**, 1493–1502.
71 J. P. Larentzos and L. J. Criscenti, *J. Phys. Chem. B*, 2008, **112**, 14243–14250.
72 N. Schwierz, *J. Chem. Phys.*, 2020, **152**, 224106.
73 D. Mammoli, N. Salvi, J. Milani, R. Buratto, A. Bornet, A. A. Sehgal, E. Canet, P. Pelupessy, D. Carnevale, S. Jannin and G. Bodenhausen, *Phys. Chem. Chem. Phys.*, 2015, **17**, 26819–26827.
74 J. M. D. Coey, *Philos. Mag.*, 2012, **92**, 1–9.
75 O. Mishima, *Proc. Jpn. Acad., Ser. B*, 2010, **86**, 165–175.